Available online at www.sciencedirect.com
ScienceDirect
International Journal of Multiphase Flow 34 (2008) 352–362
International Journal of Multiphase Flow
www.elsevier.com/locate/ijmulflow

Mixing of cohesive particles in a shear cell

Shu-San Hsiau [a,*], Li-Shin Lu [b], Cheng-Yu Chou [a], Wen-Lung Yang [a]

[a] Department of Mechanical Engineering, National Central University, No. 300, Jungda Road, Chung-Li 32001, Taiwan, ROC
[b] Department of Mechanical Engineering, Technology and Science Institute of Northern Taiwan, Taipei 11202, Taiwan, ROC

Received 9 May 2007; received in revised form 7 August 2007

Abstract

This paper discusses two series of experiments performed in a shear cell device with six different amounts of silicone oils and using 2-mm soda lime beads as the granular materials. The first series of experiments were mixing experiments, and the developments of mixing layer thicknesses were measured. The second series of experiments had the same experimental conditions as the first series but used different combinations of colored particles. In the second series of experiments, the motions of granular materials were recorded by a high-speed camera. Using the image processing technology and particle tracking method, the positions and velocities of particles were measured. The self-diffusion coefficient could be found from the history of the particle displacements.

The measured mixing layer thicknesses are compared with the calculations from a simple diffusion equation using the data of apparent self-diffusion coefficients obtained from the current measurements. The comparisons show good agreements, demonstrating that the mixing process of granular materials occur through the diffusion mechanism in this cohesive sheared flow. In addition, the apparent self-diffusion coefficient decreases with the increasing liquid volume, indicating that cohesive effect between particles reduces granular mixing.
© 2007 Elsevier Ltd. All rights reserved.

Keywords: Granular mixing; Cohesive particle; Shear cell; Self-diffusion

1. Introduction

Powder mixing has economical importance in many industries, such as pharmaceuticals, food products, ceramics, plastics, detergents, powder metallurgy, chemicals etc. For most industrial applications a better mixing process could tremendously increase the quality and the value of product. Although powder mixing is regarded as a key process, the topic has received much less attention than fluids (Ottino and Khakhar, 2000).

In order to have better design for powder mixing, the fundamentals of granular mixing and the mechanism of the process need to be studied. The rate of the mixing process and the achievable homogeneity are seriously influenced by the mixing mechanism (Gyenis, 1999). Lacey (1954) had pointed out three mixing mechanisms of dry granular materials: (i) convective mixing – the transfer of larger particle groups from one location to another, (ii) diffusive mixing – the distribution of particles over a freshly developed surface, and (iii) shear mixing – the development of slipping planes within the grain packing. From several experimental studies, it has been demonstrated that the mixing process occurred through a diffusion mechanism in different transport devices (Scott and Bridgewater, 1976; Hwang and Hogg, 1980; Buggish and Löffelmann, 1989; Zik and Stavans, 1991; Hsiau and Hunt, 1993a; Hunt et al., 1994; Natarajan et al., 1995; Hsiau and Shieh, 1999; Hsiau et al., 2005). Computer simulation, a powerful tool, was also employed to study the mixing behaviors in different granular flow systems. Cleary et al. (1998) delivered a simulation study of granular mixing to demonstrate that the amount and nature of the mixing was quite sensitive to a range of physical properties. Henrique et al. (2000) used computer simulation to examine the influence of granular temperature gradient on the mixing condition.

* Corresponding author. Tel.: +886 3 426 7341; fax: +886 3 425 4501.
E-mail address: sshsiau@cc.ncu.edu.tw (S.-S. Hsiau).

0301-9322/$ - see front matter © 2007 Elsevier Ltd. All rights reserved.
doi:10.1016/j.ijmultiphaseflow.2007.11.002

However, the existence of a small amount of interstitial fluid in the powder system may cause another degree of complexity due to the cohesive forces between particles in addition to the core repulsive force and the force of friction in a dry granular matter. It is well known that the increase in repose angle may result from the presence of interstitial fluid in a powder system (Tegzes et al., 1999; Halsey and Levine, 1998; Mason et al., 1999). The interstitial fluid also influences the powder percolation, and the powders tend to behave as clumps rather than individual grains. When the particles contain slight amount of water, they would gather together and hinder the movements by themselves. Ambient humidity, for instance, causes serious disruptions by creating clumps of particles that are more or less mobile. We know from common experience that wet sands could be fairly cohesive, whereas dry sands crumble apart readily. Due to the appearance of the liquid bridge between particles, the capillary force should be considered as an important force affecting the motion behaviors of the granular system. Calculating the capillary force that keeps two wet spheres in contact is far from trivial. Several methods have been proposed to avoid the difficulties associated with solving the Laplace–Young equation (Erle et al., 1971; Lian et al., 1993).

In past decade, the interesting effect of cohesion between grains has intrigued researchers to investigate the mixing of cohesive particles. In many instances, the cohesive nature of a powder sample is a prime factor causing difficulties in powder flowability resulting in, for example, channeling and defluidization in combustion/feeder systems. The mixing and transport properties are influenced seriously by the amount of moisture added in the granular flow. If the particles are wet, the flow becomes more viscous and liquid bridges form between particles. The dynamic liquid bridge forces are considered as cohesive forces between particles to restrict particle movements. The cohesive forces make the particles stick together with each other and hamper the movement of particles.

McCarthy et al. (2000) used computation simulation to analyze particle mixing in different geometrical drums and discovered that the liquid bridge forces between particles may increase mixing. Nase et al. (2001) modeled cohesive forces among particles and explored the cohesive strength. Based on the physical picture of liquid-induced cohesion, they proposed two discrete characterization criteria. Hsiau and Yang (2003) found that mixing rate might be increased by adding very little amount of moisture into a vibrated granular bed. Similar findings in drums were mentioned by McCarthy (2003). Jain et al. (2004) introduced Granular Capillary Number, a ratio of the capillary force to the drag force, to computationally test over a range of cohesive strengths in gas–solid flows.

The Couette granular flow is considered as one of the simplest flow models and very suitable for fundamental research. Hsiau et al. (2005) experimentally studied particle mixing in a shear cell using cohesionless soda lime beads and demonstrated that the mixing processes occurred through a diffusion mechanism. Li and McCarthy (2006) extended their previous theoretical arguments for pseudo-static particle systems to sheared granular flows and developed phase diagrams to predict cohesive particle mixing/segregation. This paper tried to study the mixing of wet sheared granular flows in a Couette shear device to understand the mechanisms of granular mixing. The results of experiments are compared with calculations from the diffusion equation.

2. Experimental setup and technique

In this study, all the experiments of granular motion are performed in a shear cell as shown in Fig. 1. The Couette shear cell is the same as the one we used in our earlier mixing experiments (Hsiau et al., 2005). It is composed of an upper disk, a bottom disk and a motor. The bottom disk, with outside diameter of 45.00 cm, is driven by a 3 hp server motor. The rotation speed was controlled by a server motor. The bottom disk was made of plexiglass for the purpose of observation. An annular trough with inside diameter of 31.67 cm, outside diameter of 42.02 cm and depth of 4.5 cm was cut in the bottom disk. A stationary upper disk could be inserted into the trough where the granular materials were put in the test section. The height of the test section $2h$ could be adjusted by moving the upper disk and be measured by a dial indicator.

We used the soda lime beads, with an average diameter d_p of 2 ± 0.09 mm and particle density of 2508 kg/m^3, as granular materials in the experiments. The soda lime beads were specially manufactured as very spherical balls with very smooth surface quality. There were two series of experiments in this study. For the first series of experiments, the mixing experiments, the same particles but with different colors are initially arranged in the top–bottom organization (top: white; bottom: black) to investigate the mixing behavior of granular materials. The total granular mass was 2.0 kg with a half in black and a half in white. The average solid fraction of the tested granular materials is calculated from the total particle mass divided by the particle density and the test section volume. The shear cell was fixed at a channel height ($2h$) of 2.16 cm, so that the average solid fraction of the test channel was a constant, 0.6163. With this solid fraction, the granular flows were very dense and had serious contacts with the upper wall. A layer of 3 mm soda lime beads was adhered to both the bottom and the top surfaces, in a random packing organization. Fig. 2 shows the image of initial situation of particles in the channel for the mixing experiments.

This paper intends to investigate the effect of adding little amount of liquid on the mixing behavior. The silicone oil, with density of 950 kg/m^3, surface tension of 2.04×10^{-2} N/m and viscosity of 50 cs (centi-stoke, cm^2/s), was added to the soda lime beads with little amount. Before each test, a certain amount of silicone oil and test particles were weighed by an electronic scale with an accuracy of 0.001 g. The silicone oil and the particles were put into a

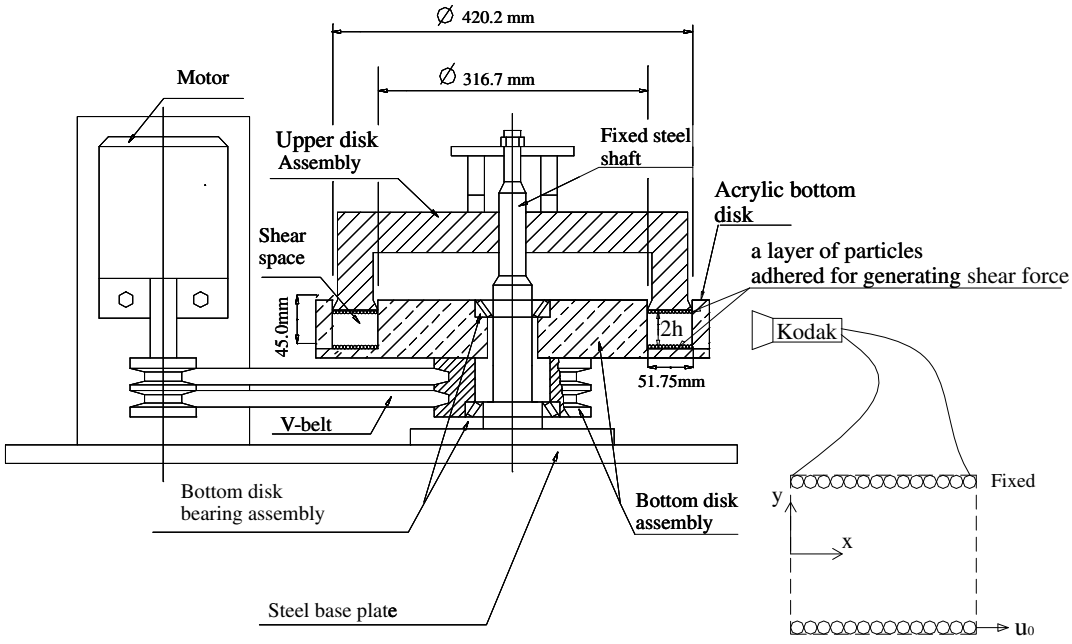

Fig. 1. The schematic drawing of the experimental Couette shear device.

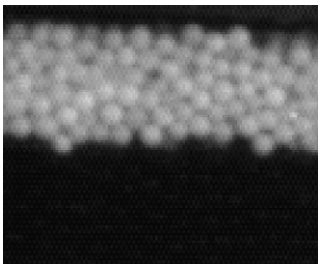

Fig. 2. Image of initial situation of particles in the channel for the mixing experiments.

sealed jar. The sealed jar was shaken to mix the silicone oil and particles. The wet particles were then put into the test section of the Couette shear device. We also measured the weight of the sealed jar and the residual silicone oil, which coherences the sealed jar. The accurate values of the masses and volumes of silicone oil and particles, which were put in the shear cell could be calculated. The dimensionless liquid volume V^* is defined by the volume of the silicone oil, added to soda lime beads, divided by the summation of the volumes of adding silicone oil and of the total soda lime beads. The current study used the dimensionless liquid volume as the controlling parameter with $V^* = 0$, 1.3×10^{-4}, 2.5×10^{-4}, 6.5×10^{-4}, $1.3 \times 10^{-3}$and 2.5×10^{-3}.

The granular flow in the test section is assumed to be two-dimensional with streamwise (horizontal) direction as x-axis and transverse (vertical) direction as y-axis (upwards is positive). Because of the limitations on observation, only the flows adjacent to the outer surface of the annular trough in the bottom disk could be recorded and analyzed. The inner surface was cleaned and polished before each experiment to reduce the wall friction effect. The velocity at the bottom (outside lower corner of the trough) u_0 could be calculated from the product of the rotational speed of the bottom disk and the outside radius of the trough. In our previous study (Hsiau et al., 2005), five bottom wall velocities u_0, 0.66 m/s (30 rpm), 0.88 m/s (40 rpm), 1.10 m/s (50 rpm), 1.32 m/s (60 rpm) and 1.54 m/s (70 rpm), were used to investigate the mixing process in a shear cell. In this study, the bottom wall velocity u_0 was chosen as 1.32 m/s in all experimental tests since the mixing phenomenon is obviously under this bottom wall velocity. From our preliminary experiments, the granular flow can be assumed as two-dimensional with negligible radial movements for this bottom wall velocity.

A Kodak motion corder analyzer, with highest speed of 10,000 frames per second, was used to record the mixing process. The frame rate of 500 frames per second, with spatial resolution of 128×120, was used in this study. The recorded images were digitized to gray levels, ranging from 0 to 255 due to the different colors of the black and the white particles, and stored in a computer file. The test section was divided into 10 regions along the transverse direction. Using image processing, the concentrations of white particles $C(t)$ in each region were determined. Fig. 3 schematically shows the development of mixing layer with time. The symbol of y denotes the vertical coordinate and $y = 0$ indicates the center of the channel. The mixing layer thickness $\delta(t)$ is defined from the width with concentrations ranging from 0.05 to 0.95. The symbols $\delta_1(t)$ and $\delta_2(t)$ denote the thicknesses of the mixing layers in the upper and the lower parts, respectively.

To investigate the diffusion process, the velocities, fluctuation velocities and self-diffusion coefficients were also determined from the second series of experiments by different

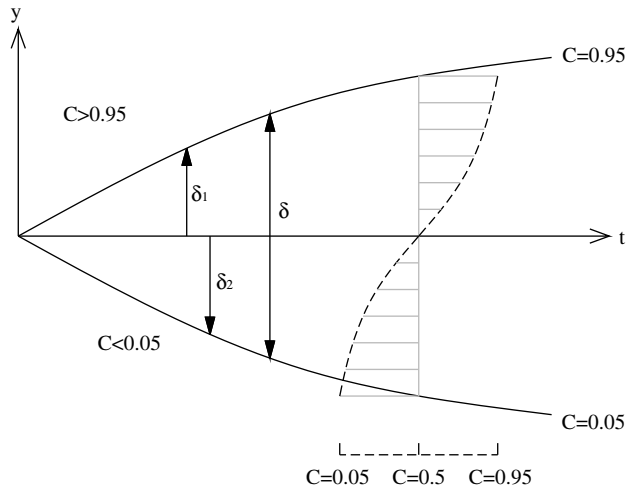

Fig. 3. Schematic representation of the mixing layer thicknesses developed in the Couette shear cell.

combinations of colored particles: The white particles (15%) served as tracer particles were mixed uniformly with black particles (85%). All the experimental settings were the same as the mixing experiment (first series of experiments), except for the amount and arrangement of colored particles. In order to measure the velocities of particles, the auto-correlation technique was employed to process the stored images and to decide the shift of each tracer particle in every two consecutive images. The details of the auto-correlation technique can be referred to our previous paper (Hsiau and Shieh, 1999). The idea of a "periodic cell" used in computer simulation was introduced in Hsiau and Shieh's experiment.

The test section was also divided into 10 regions in this series of experiment. By averaging about 250 tracer particles' velocities from approximately 8500 frames, the overall average velocities in horizontal and vertical directions, $\langle u\rangle$ and $\langle v\rangle$, in each region were determined. The fluctuation velocities in the two directions, $\langle u'^2\rangle^{1/2}$ and $\langle v'^2\rangle^{1/2}$, for each region were defined by the mean square root of the deviations of each local velocity from the overall average velocity. The granular temperature T was used to quantify the kinetic energy of the flow, and could be calculated from the average of the mean square of the fluctuation velocities in two directions:

$$T = \frac{\langle u'^2 + v'^2\rangle}{2} \tag{1}$$

Since the current study followed the auto-correlation technique developed by Hsiau and Shieh (1999) which considered the correlation values of gray level derivatives, the experimental errors of the velocities were reduced to within 1.5%.

The velocity fluctuations induce the self-diffusion in granular shear flows. Einstein (1956) first employed this concept to analyze the diffusive phenomena of suspended particles with Brownian motion in a liquid. This idea was also used by Savage and Dai (1993) and by Campbell (1997) to investigate the diffusive behavior of granular flow systems through computer simulation. The self-diffusion coefficient D_{ij} was defined as

$$\lim_{t\to\infty}\langle \Delta x_i \Delta x_j\rangle = 2D_{ij}t \tag{2}$$

where Δx_i and Δx_j are the diffusive displacements in directions i and j. A similar concept was employed in experiments by Natarajan et al. (1995) to study the granular self-diffusion in a 1-m-high vertical channel, and by Hsiau and Shieh (1999) to study the diffusion in a shear cell. In order to obtain longer histories of particle movements in a Couette device through a small camera window, the idea of "periodic cell" used in computer simulation (Campbell and Brennen, 1985) was proposed for application in experiments by Hsiau and Shieh (1999). In the periodic cell used in computer simulation, when a particle leaves the cell, a new particle with the same velocity will be set at the same transverse position in the cell inlet. Employing this idea to this experiment, when a tracer particle moved out of one image, the time counter for this particle paused until another tracer particle entered the cell inlet with the same channel height and the same velocity as the previous tracer particle. The path of this new tracer particle from the image inlet was then treated as the continuous movements of the former tracer particle. Details can be found in the paper by Hsiau and Shieh (1999), and the current study follows the same approach. Since the current mixing experiments were mainly related to the diffusion in the transverse direction, we only evaluated the transverse diffusion properties in this study. The mean square diffusive displacements in the transverse direction $\langle \Delta y \cdot \Delta y\rangle$ were averaged from about 200 tracer particles taken from 6000 to 9000 frames. The experimental errors resulted mainly from the uncertainty in determining the centroid of a particle. The errors of diffusion coefficients D_{yy} were estimated within 5%.

3. Results and discussion

3.1. Velocity

Fig. 4a shows the averaged velocity distributions of particles in the shear cell with different dimensionless liquid volumes. Please note that $y/h = 1$ and -1 denote the upper and bottom walls, respectively. Since in the channel there is no bulk motion in the transverse direction, so the measured vertical velocities, $\langle v\rangle$, are very close to 0 as expected. The streamwise velocity, $\langle u\rangle$, decreases with the channel height, and the shear rates are larger in the upper channel. For the influence of liquid amount added into the system, Fig. 4a shows that the streamwise velocity is greater for the wetter case, consistent with the results of Yang and Hsiau (2005). From the velocity profiles, there exists a "solid-like region" in the lower half of the channel with faster and more uniform streamwise velocities and a "fluid-like region" in the upper section with larger shear rate (Zhang and Campbell,

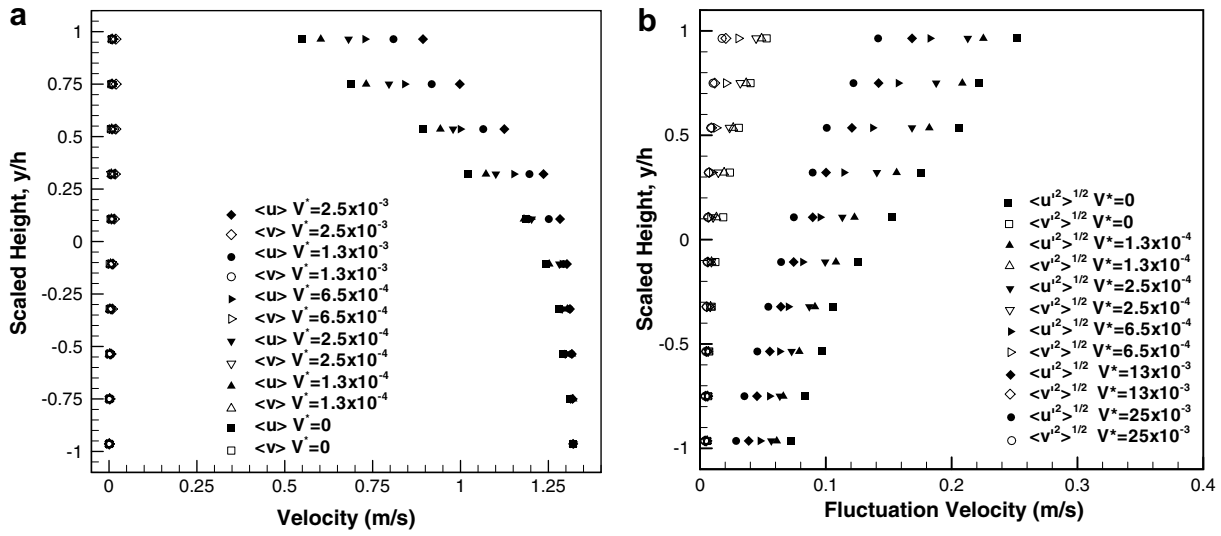

Fig. 4. The distributions of (a) overall average velocities in the streamwise ($\langle u \rangle$) and transverse ($\langle v \rangle$) directions; and (b) fluctuation velocities in the streamwise ($\langle u'^2 \rangle^{1/2}$) and transverse ($\langle v'^2 \rangle^{1/2}$) directions, with different dimensionless liquid volumes.

1992; Hsiau and Yang, 2002). From Fig. 4a, the values of the shear rate in the fluid-like region is lower for the case with greater moisture content, V^*, since the wetter particles (greater V^*) have greater cohesive forces between particles resulting in a lower velocity gradient. The energy of flow is highly dissipated due to the frictional forces, viscous force and cohesive force between particles, in a wet granular flow system. It indicates that the cohesive effect between particles inhibits particle mixing seriously.

The fluctuation velocity distributions, $\langle u'^2 \rangle^{1/2}$ and $\langle v'^2 \rangle^{1/2}$, in the channels for the six cases are shown in Fig. 4b. The fluctuations are not isotropic with the greater values in the streamwise direction. The explanation for this anisotropic phenomenon can be found in Hsiau and Shieh (1999). Due to the increasing shear rate ($\mathrm{d}\langle u \rangle/\mathrm{d}y$) with channel height indicated in Fig. 4a, the fluctuations in both directions also increase with the channel height, as shown in Fig. 4b. The effect of the moisture content on the fluctuations is significant. Both the streamwise and transverse fluctuation velocities are smaller for the wetter flow (higher V^*). The streamwise and transverse fluctuation velocities along the upper wall with zero moisture content ($V^* = 0$) are about two times and three times of those with moisture content of 2.5×10^{-3}. The deviation is mainly due to the different shear rates generated in different moisture conditions. With the greater viscous and liquid bridge forces between particles in the wetter granular flows, the flow motions are more restricted and the fluctuation velocities of the wetter granular flows are smaller.

3.2. Mixing and apparent diffusion coefficient

In this paper, the top–bottom initial loading pattern is used to investigate the particle mixing in the shear cell. Thus, the test section is also divided into two regions, the upper channel ($y > 0$) and the lower channel ($y < 0$). To examine the influence of V^* on the development of the mixing layers, the symbols in Fig. 5 shows the developments of the mixing layer thickness with time for the six tests with different liquid volumes. It is clear that the mixing layers expand with time and develop faster in the initial stages. The mixing layer thicknesses of the upper channel, δ_1, are slightly greater than those of the lower channel, δ_2. It is due to the higher fluctuations in the upper fluid-like region resulting in the higher mobility of particles for mixing. Moreover, the influence of the adding liquid amount on the development of mixing layer is significant. From this figure, the mixing layer thicknesses are greater for the dryer cases. For the dryer system containing lower liquid content, the particle fluctuations are higher, promoting the sys-

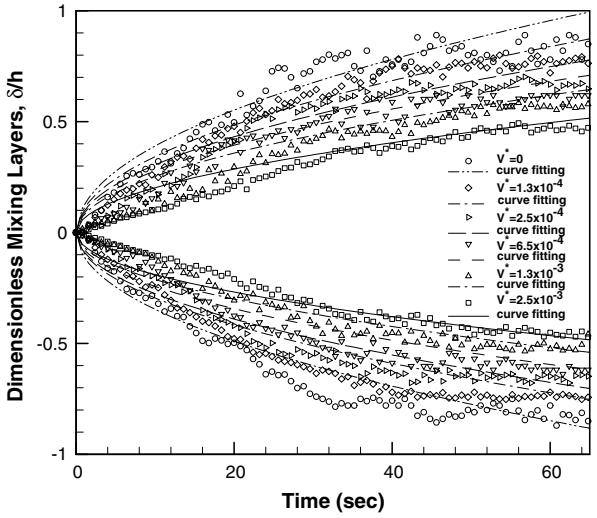

Fig. 5. The evolution of the experimental mixing layer thicknesses (symbols) with the six tests ($V^* = 0$, 1.3×10^{-4}, 2.5×10^{-4}, 6.5×10^{-4}, $1.3 \times 10^{-3}$and 2.5×10^{-3}). Curves are best fit to analytical solution described as Eqs. (6) and (7).

tem mixing, and hence the mixing layer development becomes faster.

Under the high solid fraction condition: 0.6163, particle collision is dominant to decide particle movement. In fact, the dominant mechanism affecting the flow behavior of granular materials is the random motions of particles resulting from the interactive collisions between particles (Campbell, 1990). Diffusive mixing is caused by the random motion of the individual particles, and granular mixing is mainly resulted from the diffusive motions of granular materials in the shear cell (Buggish and Löffelmann, 1989). Because of the top–bottom organization of different-colored particles, the particle mixing mostly occurred in the vertical direction. Assuming one-dimensional diffusion in the shear granular flow, the diffusion equation can be expressed as

$$\frac{\partial C}{\partial t} = \frac{\partial}{\partial y}\left(D_{yy}\frac{\partial C}{\partial y}\right) \tag{3}$$

where C and D_{yy} are the concentration of white particles, and the transverse self-diffusion coefficient. With our top-white/bottom-black particle initial organization, the initial conditions for Eq. (3) can be set as: $C = 1$ when $t = 0$, $y > 0$; and $C = 0$ when $t = 0$, $y < 0$. From Fig. 5, the growths of mixing layer thicknesses become relatively slow after a certain time. Even with longer observation of the mixing process up to a half hour, the mixing layer cannot reach the boundary walls. Thus it is reasonable to assume the boundary conditions for the above equation as: $C \to 1$ as $y \to \infty$; and $C \to 0$ as $y \to -\infty$. The transverse self-diffusion coefficients D_{yy} is actually varied with the height of the channel and will be investigated later. Here we define apparent self-diffusion coefficients, $D_{\mathrm{app},1}$ and $D_{\mathrm{app},2}$, to respectively denote the "averaged" self-diffusion in the upper and lower channels. For simplicity to derive the analytical solution to the first order, D_{yy} in Eq. (3) can be assumed as constants, $D_{\mathrm{app},1}$ and $D_{\mathrm{app},2}$, to explore the bulk mixing behavior in the upper and lower channels. Then we can solve Eq. (3) for the upper channel, $y \geqslant 0$, and lower channel, $y \leqslant 0$ with one additional boundary condition by assuming $C \to 0.5$ at $y = 0$. The analytical solutions are:

$$C(t,y) = \frac{1}{2} + \frac{1}{2}\mathrm{erf}\left(\frac{y}{2\sqrt{D_{\mathrm{app},1}t}}\right) \quad \text{(for upper channel)} \tag{4}$$

$$C(t,y) = \frac{1}{2} - \frac{1}{2}\mathrm{erf}\left(\frac{y}{2\sqrt{D_{\mathrm{app},2}t}}\right) \quad \text{(for lower channel)} \tag{5}$$

Next we use the definition of mixing layer thickness in the experiments, $C = 0.95$ at $y = \delta_1$ and $C = 0.05$ at $y = -\delta_2$, that gives

$$\delta_1 = 2.53\sqrt{D_{\mathrm{app},1}t} \quad \text{(for upper channel)} \tag{6}$$

$$\delta_2 = 2.53\sqrt{D_{\mathrm{app},2}t} \quad \text{(for lower channel)} \tag{7}$$

The fitted curves in Fig. 5 are the results of least-squares fits using the forms of Eqs. (6) and (7), indicating close correspondence with the experimental data. The deviations between fitted curves and experimental data are mainly due to the assumption of constant self-diffusion coefficients in the upper and lower channels employed in the diffusion equation.

The values of the apparent diffusion coefficients can be determined from the fitted curves, Eqs. (6) and (7), from Fig. 5. The apparent diffusion coefficients are plotted against the dimensionless liquid volume both in the upper and lower channels in Fig. 6. The results show that the increase of liquid volume in granular system causes the decrease of D_{app}, i.e., the worse mixing. The apparent self-diffusion coefficient also has greater values in the upper channel than in the lower channel, denoting a better mixing in the upper channel where the mixing layer thicknesses are thicker. The apparent self-diffusion coefficient D_{app} derived from the above means is an appropriable index to describe the bulk granular mixing condition in the shear cell.

It is interesting to discuss more about the mixing growing rate. All curves in Fig. 5 show that the mixing layer thicknesses in both upper and lower channels develop much faster in the beginning stages, and then grow smoothly. We can estimate the mixing growing rates by differentiating the mixing layer thicknesses (δ_1 and δ_2) with respect to time, according to the experimental data in Fig. 5. Fig. 7a, b show the mixing growing rates of the upper and lower channels plotted against time for the different tests. It demonstrates that the mixing rates are faster in the initial stage. The mixing rates in the upper channel (Fig. 7a) are greater than those in the lower channel (Fig. 7b) since the fluid-like behavior of the granules in the upper channel promote the granular mixing. One most important conclusion from Fig. 7a, b is that the mixing growing rates of the dryer cases are higher than those of the wetter cases.

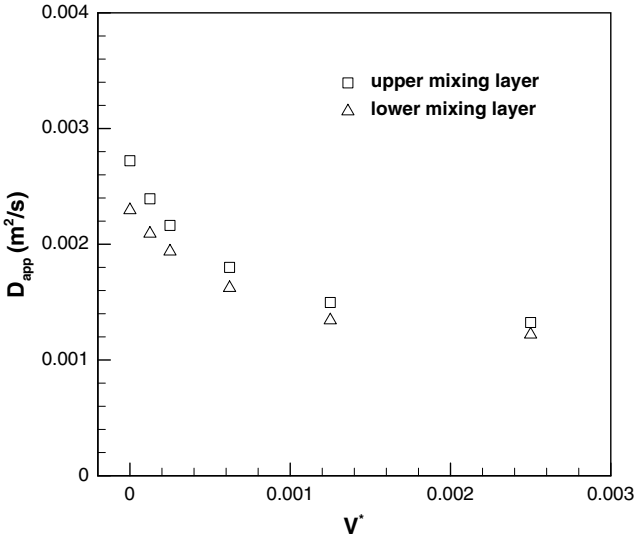

Fig. 6. The dependence of the apparent diffusion coefficient D_{app} on the dimensionless liquid volume V^* both in the upper and lower channels.

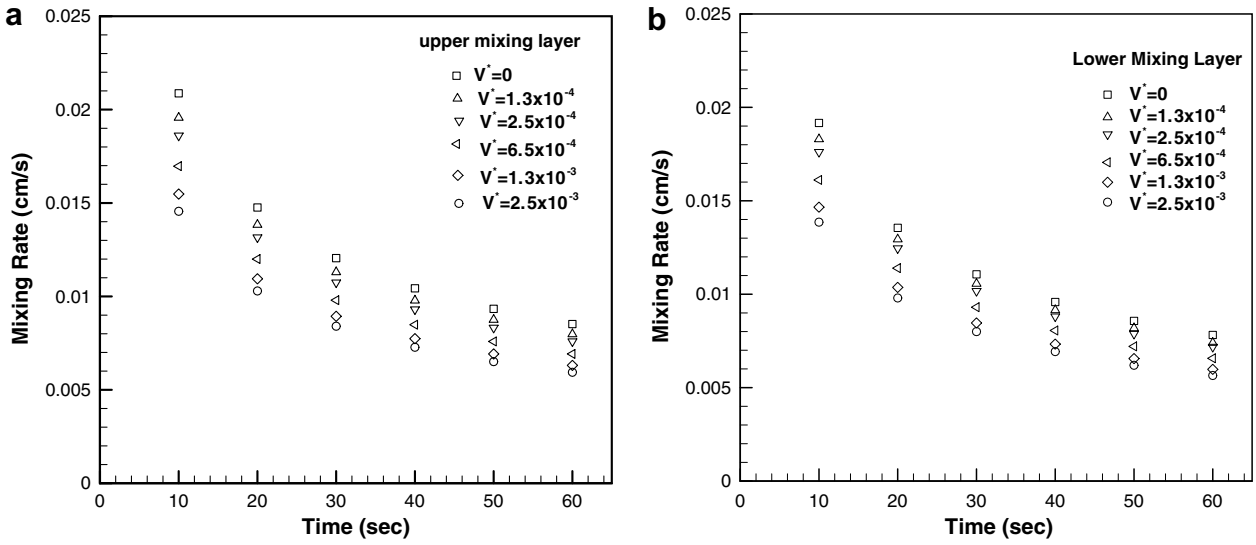

Fig. 7. The mixing growing rates varied with time for six different dimensionless liquid volumes (a) in the upper channel, (b) in the lower channel.

Granular temperature is defined as the mean square of fluctuation velocities in three directions. It physically denotes the specific kinetic energy of granular system and plays a similar role as temperature in general gases. The mixing in granular flow is related to the diffusive motions which influenced by particles' random motions. Thus, the mixing status and diffusive motions of granular materials are related to the granular temperature. Fig. 8 shows the apparent self-diffusion coefficients plotted against the square root of the average granular temperature in the vertical direction, $T_y^{1/2}, T_y = \langle v'^2 \rangle$, in the upper and lower channels, where the granular temperatures are measured from all the tests with different liquid contents. From the symbols which represent different liquid contents, both the square root of transverse granular temperatures $T_y^{1/2}$ and apparent diffusion coefficients D_{app} increase with the decrease of liquid amount. The trends have already demonstrated in Figs. 3b and 5. One important finding is that the apparent diffusion coefficient D_{app} increases linearly and significantly with the square root of the vertical granular temperature in the upper and lower channels. From the development of dense-gas kinetic theory by Hsiau and Hunt (1993b) and Savage and Dai (1993), this linear dependence relation was also indicated, although there was an assumption of isotropic granular temperature.

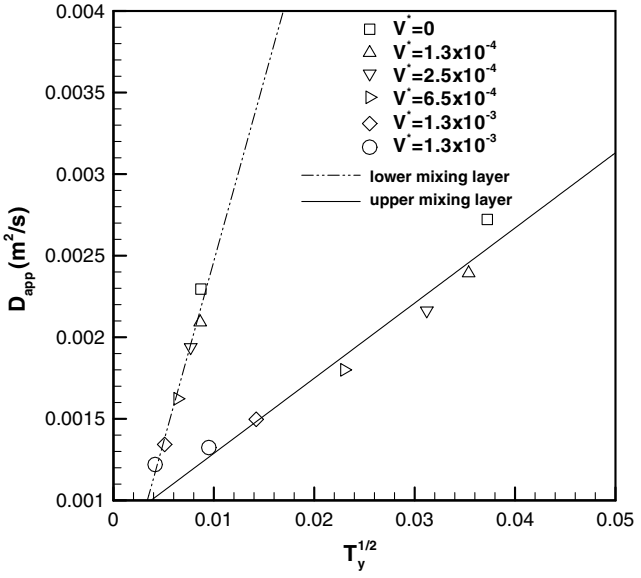

Fig. 8. The apparent self-diffusion coefficients versus the square root of the average granular temperature in the vertical direction, $T_y^{1/2}$, in the upper and lower channels.

Hsiau and Yang (2002) demonstrated that the granular temperature and the diffusion coefficient are mainly influenced by the shear rate along the (upper) wall. The values of shear rates along the upper wall could be determined by extracting data of horizontal velocity distributions in Fig. 4a. The apparent self-diffusion coefficient of the upper channel were plotted against the shear rate along the upper wall, $\langle \mathrm{d}u/\mathrm{d}y \rangle_w$, with different V^* in Fig. 9. The value of the shear rate is greatest in the test with dry granular materials. Since the higher shear rate induces stronger fluctuations and diffusion hence the greater apparent self-diffusion coefficient, as shown in Fig. 9. The apparent diffusion coefficient shows a good linear correlation with the shear rate.

3.3. Self-diffusion coefficient

Eqs. (4)–(7) are the solutions of diffusion equation, Eq. (3), based on constant-diffusion-coefficient assumption. However, Hsiau and Shieh (1999) and Hsiau and Yang (2002) demonstrated that the self-diffusion coefficient was varied with the height. Following the particle tracking method employing periodical-cell idea developed by Hsiau and Shieh (1999), we measured the transverse self-diffusion coefficients D_{yy} for all the tests, but using different initial

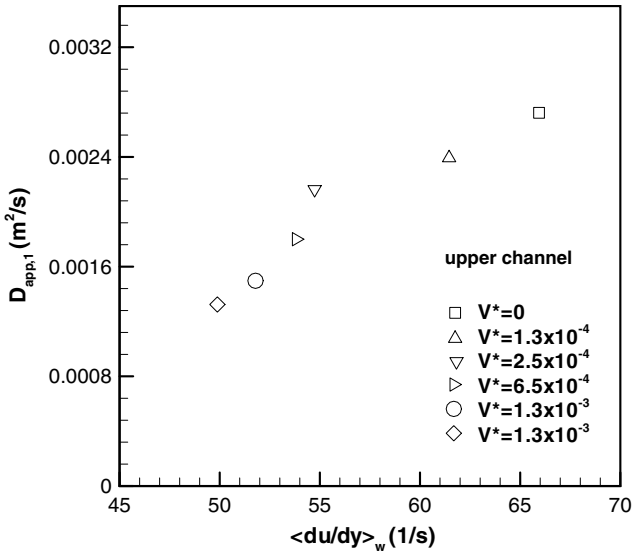

Fig. 9. The apparent self-diffusion coefficient $D_{\mathrm{app},1}$ in the upper channel versus the shear rate along the upper wall, $(\mathrm{d}\langle u\rangle/\mathrm{d}y)_w$ with six dimensionless liquid volumes.

setting of colored soda lime beads. Fig. 10 shows the distributions of the transverse self-diffusion coefficient in the test channel with V^*. The self-diffusion coefficients in the upper region ($y > 0$) are much greater than those in the lower channel ($y < 0$). In the lower channel, the variations of D_{yy} with channel height are not significant. Resulted from the gravity effect, the particles in the lower part are pressed by greater gravitational force from the upper particles and behave as solid-like and the granular structures are denser. In the upper channel, from Fig. 4a, b, there exist greater fluctuations and shear rates which induce the stronger diffusion. Fig. 10 also demonstrates that the transverse diffusion coefficient D_{yy} increases with the decreasing V^*. With more liquid added into the system, the flow becomes more cohesive with higher liquid bridge force and viscous force. The effect retards the random motions of particles and hence reduces the diffusion of particles (Yang and Hsiau, 2005).

Now we discuss some important dimensionless parameters influencing the wet granular flows. The Granular Bond Number Bo_{g} could be defined as the ratio of the maximum capillary force F_{c} and the weight of the particle, W (Nase et al., 2001):

$$Bo_{\mathrm{g}} = \frac{F_{\mathrm{c}}}{W} = \frac{2\pi R\gamma}{\frac{4}{3}\pi R^3 \rho_p g} = \frac{3\gamma}{2R^2\rho_p g} \tag{8}$$

where R is the radius of particle, γ is the surface tension of silicone oil, and ρ_p is the density of the solid. In this study, $R = 0.001$ m, $\gamma = 2.04 \times 10^{-2}$ N/m and $\rho_p = 2508$ kg/m^3, hence the Granular Bond Number is a constant, $Bo_{\mathrm{g}} = 1.24$, according to Eq. (8). For Granular Bond Number greater than 1 ($Bo_{\mathrm{g}} > 1$), the cohesive effect becomes important (McCarthy, 2003). Besides, the Collision Number Co could be defined as the ratio of the maximum capillary force F_{c} and the collisional force F_{Bg},

$$Co = \frac{F_{\mathrm{c}}}{F_{Bg}} = \frac{2\pi R\gamma}{\pi\rho_p\lambda^2 R^4\left(\frac{\mathrm{d}\langle u\rangle}{\mathrm{d}y}\right)^2} \tag{9}$$

where λ^2 is a constant equal to one and $d\langle u\rangle/dy$ represents the shear rate. The degree of collision could be determined from the Collision Number which may be calculated by using the measured shear rate, from Fig. 4a. Fig. 11 shows the relations of transverse diffusion coefficients D_{yy} versus the Collision Number Co. All the data were plotted for different section heights in all the tests with different V^*. It indicates that the transverse diffusion coefficients decrease with the increase of Collision Number with significantly correlated relations. In the upper channel with higher shear rates, the transverse diffusion coefficients are greater

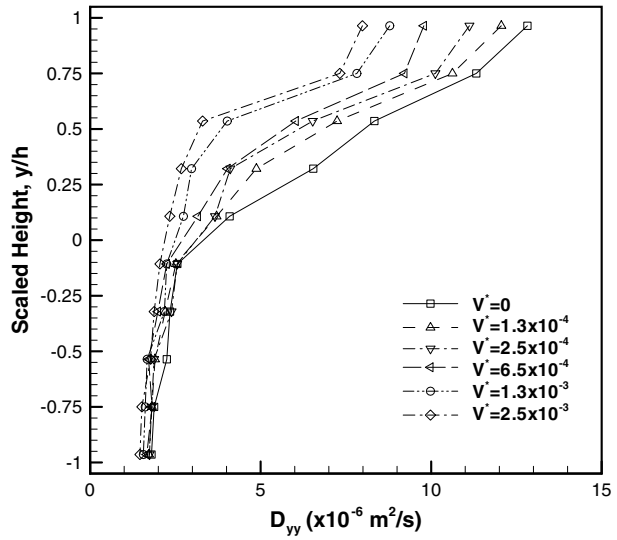

Fig. 10. The distributions of the experimental transverse self-diffusion coefficient D_{yy} with six dimensionless liquid volumes.

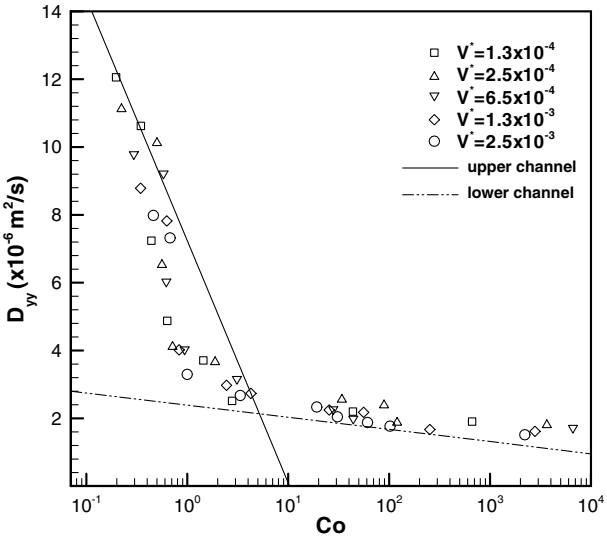

Fig. 11. The relations of transverse diffusion coefficients D_{yy} versus the Collision Number Co.

(Fig. 4a) but the Collision Numbers are smaller (Eq. (9)). From Fig. 11, the Collision Numbers are smaller than 10 in the upper channel. The power relation of

$$D_{yy} \propto Co^{-0.44} \tag{10}$$

was found for the upper channel. However, the decrease of D_{yy} with increasing Co remains but not as significant as the upper channel. The power relation becomes:

$$D_{yy} \propto Co^{-0.04} \tag{11}$$

As mentioned earlier, the self-diffusion coefficient from dense-gas kinetic theory was found to be proportional to the square root of granular temperature (Fig. 8). From the study of Campbell and Brennen (1985), the square root of granular temperature is proportional to shear rate. Since the above two relations are based on isotropic assumptions, so we only use the self-diffusion coefficient and granular temperature in transverse direction, and find that the transverse diffusion coefficient is proportional to shear rate. With the definition of Collision Number in Eq. (9), the power relation of

$$D_{yy} \propto Co^{-0.5} \tag{12}$$

is demonstrated. Due to some critical assumptions were invalid in a practical granular flow, the experimental finding for the upper channel (Eq. (10)) has little deviation from the ideal theory. However for the lower channel, the flow regime belongs to "solid-like" where the dense-gas kinetic theory is not able to well describe the flow. Thus the experimental result in Eq. (11) deviates the theoretical relation very much.

3.4. Concentration profiles

At last, we will present the concentration profiles. We had solved diffusion equation Eq. (2) by substituting the

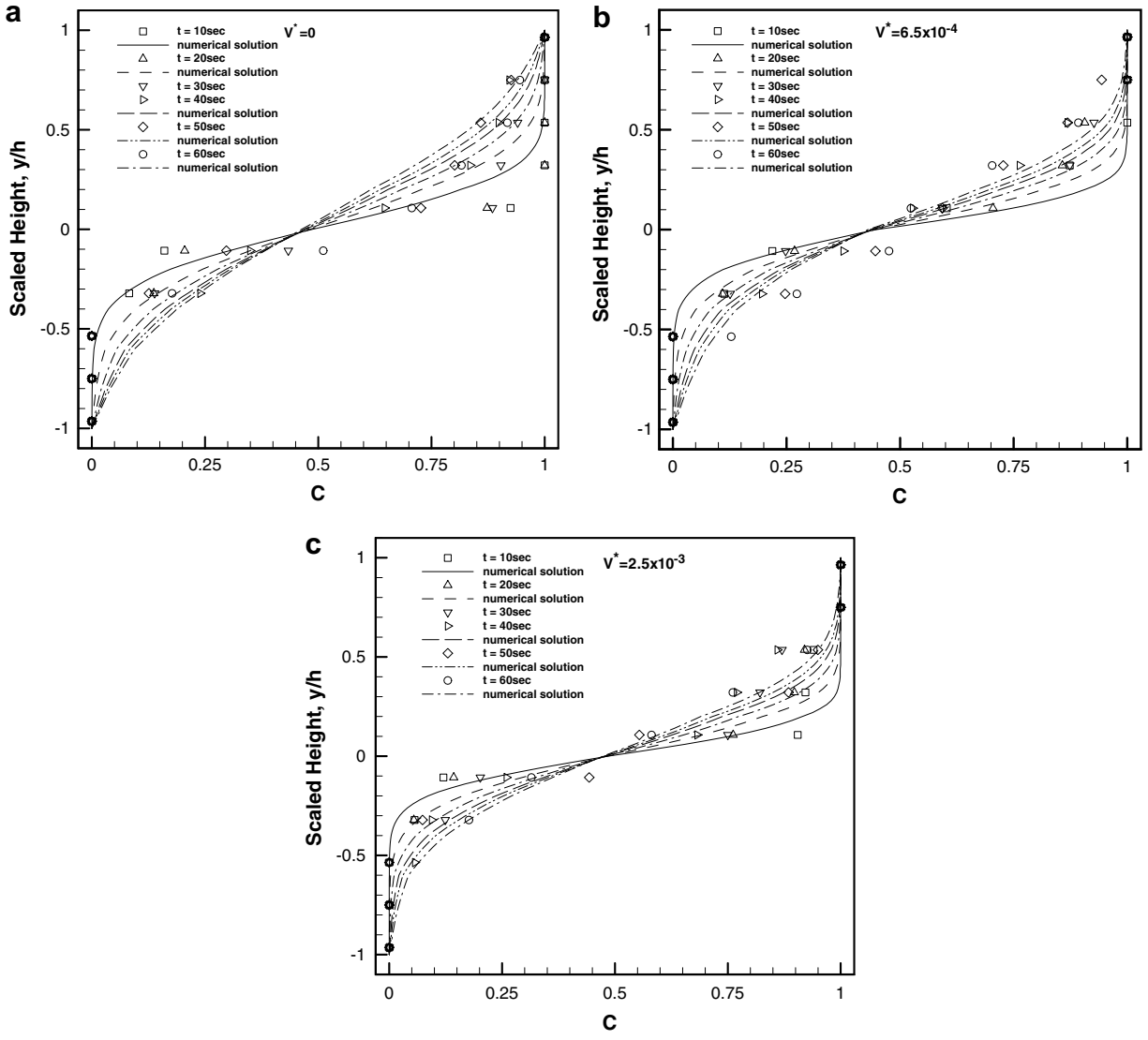

Fig. 12. The concentration distributions of both the experimental measurements (symbols) and the numerical solutions (curves) at times of 10, 20, 30, 40, 50 and 60 s: (a) $V^* = 0$, (b) $V^* = 6.5 \times 10^{-4}$, (c) $V^* = 2.5 \times 10^{-3}$.

apparent diffusion coefficient. For a much better accuracy, we may use the experimental measurements of the transverse diffusion coefficients $D_{yy}(y/h)$ (Fig. 10) and solve the diffusion equation by the finite difference method. The initial conditions are the same as the previous ones, while the boundary conditions are

$$\left(\frac{\partial C}{\partial y}\right)_{y=\pm h} = 0 \tag{13}$$

since the mass flux through the walls is zero. Hence the concentration $C(y/h)$ can be calculated from the finite difference equations. Fig. 12a–c show the concentration distributions in the channel at times of 10, 20, 30, 40, 50 and 60 s, from both the experimental measurements and the numerical solutions for V^* of 0, 6.5×10^{-4}, 2.5×10^{-4}. Generally, a perfect mixing condition means that the concentrations in all levels are 0.5, although this is almost impossible in an actual situation. Therefore, the smaller concentration gradient in the channel indicates that the mixture is more homogeneous with better mixing conditions. From these figures, the higher liquid content V^* results in a larger concentration gradient along the height. It indicates that the higher liquid content V^* causes worse mixing in the channel. Fig. 12a–c also show the deviations between experiments and numerical results are larger in the central channel, which is due to the difficulty in determining the concentration accurately in this region.

The semi-theoretical mixing layer thickness can be calculated by the combination of the numerical solutions of concentration along the height and the definition of the mixing layer thickness, as mentioned above. Fig. 13 shows the semi-theoretical results compared with the experimental data for the mixing layer thickness non-dimensionalized by the half channel height. The comparison shows a very good agreement, indicating that the mixing process of wet granular materials in the shear cell occurred throughout the diffusion mechanism.

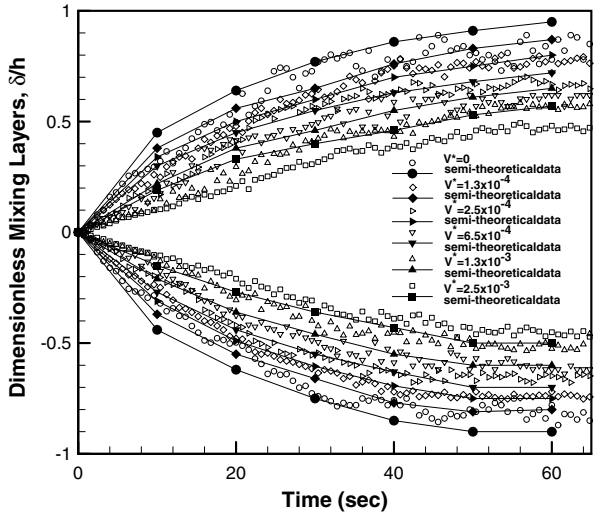

Fig. 13. The semi-theoretical results (closed symbols with lines) compared with the experimental results (open symbols) of the evolution of the mixing layer thicknesses under six dimensionless liquid volumes.

4. Conclusions

In this paper, the effects of adding liquid into sheared granular flows on the mixing process and movements of granular materials were investigated. In the wetter granular flows where cohesive forces and viscous force exist, the fluctuations, the shear rates and the self-diffusion coefficients are smaller. The apparent self-diffusion coefficients, denoting the averaged self-diffusion coefficients, were found to increase with the decrease of liquid volume. This study also demonstrated that the apparent self-diffusion coefficients linearly increase with the increases of the square root of transverse granular temperature and the shear rate along the upper wall.

The self-diffusion coefficient was measured at different channel height. The semi-theoretical results, by substituting the measured self-diffusion coefficients into the diffusion equation, agree well with the experimental data, demonstrating that the cohesive particle mixing in the sheared granular flow is governed by the diffusive mechanism.

Acknowledgement

Financial support by the National Science Council of the ROC for this work through projects NSC 95-2212-E-008-061 and NSC 95-2221-E-008-135-MY2 is gratefully acknowledged.

References

Buggish, H., Löffelmann, G., 1989. Theoretical and experimental investigation into local granulate mixing mechanism. Chem. Eng. Process. 26, 193–200.

Campbell, C.S., 1990. Rapid granular flows. Ann. Rev. Fluid Mech. 22, 57–92.

Campbell, C.S., 1997. Self-diffusion in granular shear flows. J. Fluid Mech. 348, 85–101.

Campbell, C.S., Brennen, C.E., 1985. Computer simulation of granular shear flows. J. Fluid Mech. 151, 167–188.

Cleary, P.W., Metcalfe, G., Liffman, K., 1998. How well do discrete element granular flow models capture the essentials of mixing processes. Appl. Math. Model. 22, 995–1008.

Einstein, A., 1956. Investigations on the Theory of Non-Uniform Gases. Dover Publications, New York, Chapter 1, 12–27.

Erle, M.A., Dyson, D.C., Morrow, N.R., 1971. Liquid bridge between cylinders, in a torus, and between spheres. AIChE J. 17, 115–121.

Gyenis, J., 1999. Assessment of mixing mechanism on the basis of concentration pattern. Chem. Eng. Process. 38, 665–674.

Halsey, T.C., Levine, A.J., 1998. How sandcastles fall. Phys. Rev. Lett. 80, 3141–3144.

Henrique, C., Batrouni, G., Bideau, D., 2000. Diffusion as a mixing mechanism in granular materials. Phys. Rev. E 6301, 1304–1311.

Hsiau, S.S., Hunt, M.L., 1993a. Shear-induced particle diffusion and longitudinal velocity fluctuations in a granular-flow mixing layer. J. Fluid Mech. 251, 299–313.

Hsiau, S.S., Hunt, M.L., 1993b. Kinetic theory analysis of flow-induced particle diffusion and thermal conduction in granular material flows. J. Heat Transfer 155, 541–548.

Hsiau, S.S., Shieh, Y.H., 1999. Fluctuations and self-diffusion of sheared granular material flows. J. Rheol. 43, 1049–1066.

Hsiau, S.S., Yang, W.L., 2002. Stresses and transport phenomena in sheared granular flows with different wall conditions. Phys. Fluids 14, 612–621.

Hsiau, S.S., Yang, S.C., 2003. Numerical simulation of self-diffusion and mixing in a vibrated granular bed with the cohesive effect of liquid bridges. Chem. Eng. Sci. 58, 339–352.

Hsiau, S.S., Lu, L.S., Chen, J.C., Yang, W.L., 2005. Particle mixing in a sheared granular flow. Int. J. Multiphase Flow 31, 793–808.

Hunt, M.L., Hsiau, S.S., Hong, K.T., 1994. Particle mixing and volumetric expansion in a vibrated granular bed. J. Fluids Eng. 116, 785–791.

Hwang, C.L., Hogg, R., 1980. Diffusive mixing in flowing powders. Powder Technol. 26, 93–101.

Jain, K., Shi, D., McCarthy, J.J., 2004. Discrete characterization of cohesion in gas–solid flows. Powder Technol. 146, 160–167.

Lacey, P.M.C., 1954. Developments in the theory of particle mixing. J. Appl. Chem. 4, 257–268.

Li, H., McCarthy, J.J., 2006. Cohesive particle mixing and segregation under shear. Powder Technol. 164, 58–64.

Lian, G., Thornton, C., Adams, M.J., 1993. A theoretical study of the liquid bridge forces between two rigid spherical bodies. J. Colloid Interface Sci. 161, 138–147.

Mason, T.G., Levine, A.J., Ertas, D., Halsey, T.C., 1999. Critical angle of wet sandpiles. Phys. Rev. E 60, R5044–R5047.

McCarthy, J.J., 2003. Micro-modeling of cohesive mixing processes. Powder Technol. 138, 63–67.

McCarthy, J.J., Khakhar, D.V., Ottino, J.M., 2000. Computational studies of granular mixing. Powder Technol. 109, 72–82.

Nase, S.T., Vargas, W.L., Abatan, A.A., McCarthy, J.J., 2001. Discrete characterization tools for cohesive granular material. Powder Technol. 116, 214–223.

Natarajan, V.V.R., Hunt, M.L., Taylor, E.D., 1995. Local measurements of velocity fluctuations and diffusion coefficients for a granular material flow. J. Fluid Mech. 304, 1–25.

Ottino, J.M., Khakhar, D.V., 2000. Mixing and segregation of granular materials. Ann. Rev. Fluid Mech. 32, 55–91.

Savage, S.B., Dai, R., 1993. Studies of granular shear flows: wall slip velocities, 'layering' and self-diffusion. Mech. Mater. 16, 225–238.

Scott, A.M., Bridgewater, J., 1976. Self-diffusion of spherical particles in a simple shear apparatus. Powder Technol. 14, 177–183.

Tegzes, P., Albert, R., Paskvan, M., Barabási, A.L., Vicsek, T., Schiffer, P., 1999. Liquid-induced transitions in granular media. Phys. Rev. E 60, 5823–5826.

Yang, W.L., Hsiau, S.S., 2005. Wet granular materials in sheared flows. Chem. Eng. Sci. 60, 4265–4274.

Zhang, Y., Campbell, C.S., 1992. The interface between fluid-like and solid-like behaviour in two-dimensional granular flows. J. Fluid Mech. 237, 541–568.

Zik, O., Stavans, J., 1991. Self-diffusion in granular flows. Europhys. Lett. 16, 255–258.